

## Article

# Two Mechanisms of Earthquake-Induced Hydrochemical Variations in an Observation Well

Zhihua Zhou <sup>1,\*</sup> , Jun Zhong <sup>1</sup>, Jing Zhao <sup>1,2</sup>, Rui Yan <sup>1</sup>, Lei Tian <sup>1</sup> and Hong Fu <sup>3</sup>

<sup>1</sup> China Earthquake Networks Center, Beijing 100045, China; zjadvance@126.com (J.Z.); zhaozhengjia1@126.com (J.Z.); yanrui@seis.ac.cn (R.Y.); leitian@seis.ac.cn (L.T.)

<sup>2</sup> Institute of Geology, China Earthquake Administration, Beijing 100029, China

<sup>3</sup> Yunnan Earthquake Agency, Kunming 650225, China; ynfuhong@263.net

\* Correspondence: basalin@hotmail.com

**Abstract:** Due to frequent large earthquakes in the Lanping-Simao fault basin—located in China’s Yunnan Province—the Simao observation well has observed groundwater discharge, as well as  $\text{Ca}^{2+}$ ,  $\text{Mg}^{2+}$ , and  $\text{HCO}_3^-$  concentrations every day between 2001–2018. Over 18 years of observations,  $M \geq 5.6$  earthquakes within a radius of 380 km from the well were seen to cause hydrochemical variations. In this study, we investigated  $\text{CO}_2$  release and groundwater mixing as possible causes of regional earthquake precursors, which were caused by the characteristics of the regional structure, lithology, water-rock reactions, and a GPS velocity field. Precursory signals due to  $\text{CO}_2$  injection are normally short-term changes that take two months. However, groundwater mixing linked to earthquakes was found to take, at the earliest, 15 months. The proportion of shallow water that contributes to mixing was found to significantly increase gradually with the stronger regional strain. These findings delineate the two mechanisms of earthquake-induced hydrochemical variations in an observation well, and would contribute to a better understanding of chemical changes before events in the Simao basin.

**Keywords:** hydrochemistry; earthquake precursor;  $\text{CO}_2$  injection; groundwater mixing; long-term observation well



**Citation:** Zhou, Z.; Zhong, J.; Zhao, J.; Yan, R.; Tian, L.; Fu, H. Two Mechanisms of Earthquake-Induced Hydrochemical Variations in an Observation Well. *Water* **2021**, *13*, 2385. <https://doi.org/10.3390/w13172385>

Academic Editor: Thomas Meixner

Received: 27 July 2021

Accepted: 27 August 2021

Published: 30 August 2021

**Publisher’s Note:** MDPI stays neutral with regard to jurisdictional claims in published maps and institutional affiliations.



**Copyright:** © 2021 by the authors. Licensee MDPI, Basel, Switzerland. This article is an open access article distributed under the terms and conditions of the Creative Commons Attribution (CC BY) license (<https://creativecommons.org/licenses/by/4.0/>).

## 1. Introduction

Earthquake-induced geochemical processes are complex natural phenomena. Many earthquakes occur in areas where underground fluids are inaccessible; however, the hydrochemical constituents are important parameters that can provide precursory information [1,2]. The chemical composition of groundwater provides information about fluid transfer during crustal deformation, while gases can provide information about deep fluid migration towards the Earth’s surface [3,4]. Since the 1960s, numerous studies have reported changes in groundwater chemistry before earthquakes over wide temporal and spatial ranges [5–11].

There are many reasons for earthquake precursors at sites both proximal and distal to an epicenter, including the increased injection of deep-trapped  $\text{CO}_2$  into aquifers, the mixing of groundwater components in response to crustal dilation, dilation due to increasing numbers and sizes of microcracks, the squeezing of gas-rich pore fluids out of the rock matrix and into aquifers, increased rock/water interactions, and permeability dominant with increasing lithostatic load [12–20]. Earthquake-related changes at sensitive sites are usually similar for different earthquakes, regardless of the earthquakes’ locations and focal mechanisms [21–27]. Some areas have hosted experimental monitoring activities in geofluids oriented to geodynamic monitoring and to research about possible earthquake precursors [28], especially in China. However, the research of mechanisms driving changes are still not enough [2,29]. Therefore, it is necessary to research the repeated response before

strong events to better understand chemical change mechanisms in long-term continuous hydrochemical observations.

The Lanping-Simao fault basin, located in southwest China in the Yunnan Province, has both a complex geological structure and frequent earthquakes of  $M \geq 6$  [30]. Previous work has shown that CO<sub>2</sub> release and groundwater mixing due to pre-seismic tectonic movement both occur in this region [31]. Geochemical observations are known to be sensitive to pre-seismic CO<sub>2</sub> release and groundwater mixing [4,32]. The long-term monitoring of ion concentrations in observation wells can reveal the precursory signals of earthquakes [1,11,33,34]. In this study, we used 18 years of observation data from the Simao groundwater observation well to comprehensively analyze the precursory characteristics of  $M \geq 5.6$  earthquakes within a radius of 380 km. In this study, we focused on long-term hydrochemical characteristics caused by two genetic mechanisms: CO<sub>2</sub> injection and groundwater mixing. Herein, we attempted to decipher possible hydrochemical precursory signals in Simao basin.

## 2. Geological Setting

The Lanping-Simao fault basin is a seismically active thrust and strike-slip fault zone formed by the collision and continuous compression between the Indian and Eurasian tectonic plates [35]. The basin has a tectonic association with continental rift volcanism and an abundance of geothermal hot springs [36,37]. During the Himalayan Orogeny (68–23 Ma), a number of alkaline magmatic intrusions with mantle enclaves formed within the basin [38–40]. This directly led to an abundance of CO<sub>2</sub>-rich fluid inclusions, and CO<sub>2</sub> release may be an important precursory phenomenon. Based on CO<sub>2</sub>/<sup>3</sup>He, <sup>3</sup>He/<sup>4</sup>He, and <sup>13</sup>C<sub>CO2</sub> isotopic evidence, hydrothermal gases (CO<sub>2</sub>) from the Simao basin are originally sourced from deeper within the mantle [41]. Although sandstone-type orebodies are stratiform, mineralization is best developed close to regional faults [42]. Gangue minerals are mainly quartz and calcite [40]; carbonization is common in the schistosity zone, reflecting brittle tectonic deformation [43]. The water yield property is quite different in the basin. The carbonate rock area in the middle and edge of the basin is dominated by karst water, and the basin is dominated by structural fissure water and dissolved pore water in a large range. It is easy to enrich structural fissure water in the fault fracture zone along the fault. Furthermore, there are many interlayer water storage layers with frequent alternation of aquifers and aquifers. This leads to easy mixing of groundwater with different chemistries [37]. Groundwater comes from atmospheric precipitation and the recharge elevation is about 1257–2351 m by the results of hydrogen and oxygen isotopic composition. Moreover, the hot spring circulation depth in the basin is about 1123–3443 m deep, according to the quartz thermometric scale [37].

The Simao observation well (101.05° E, 22.73° N) was established for seismic monitoring and earthquake prediction (Figure 1). It is a water well with a depth of 112.27 m. The casing section extends to 26.69 m, and the sampling water is a mixture of inputs from multiple aquifers at depths between 26.69 and 110.76 m. It is fracture-confined water and the flow rate is 0.3–0.6 L/s [44]. The water yield property is high [45]. The lithology of the main aquifer is gray-green medium–thick quartz clastic sandstone with calcite dikes; its hydrochemical type is HCO<sub>3</sub>-Ca·Na. Silty mudstone at a depth of 14.03–26.69 m provides an overlying impermeable layer, and so the aquifer is seldom affected by seasonal rainfall. A gray-green tuffaceous mudstone at a depth of 110.76 m provides a barrier with a deeper aquifer (Figure 2).

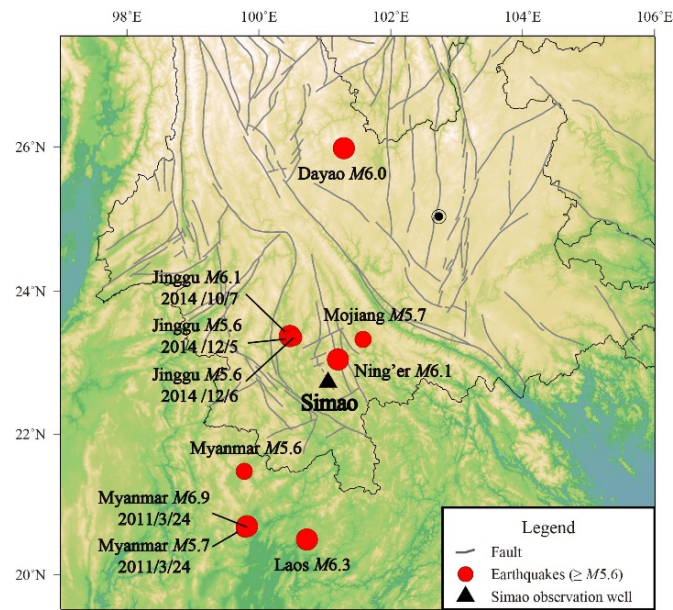


**Figure 1.** Location of the Simao observation well, Yunnan Province, China. Red circles denote earthquakes of  $M \geq 5.6$  within a radius of 380 km (2001–2018).

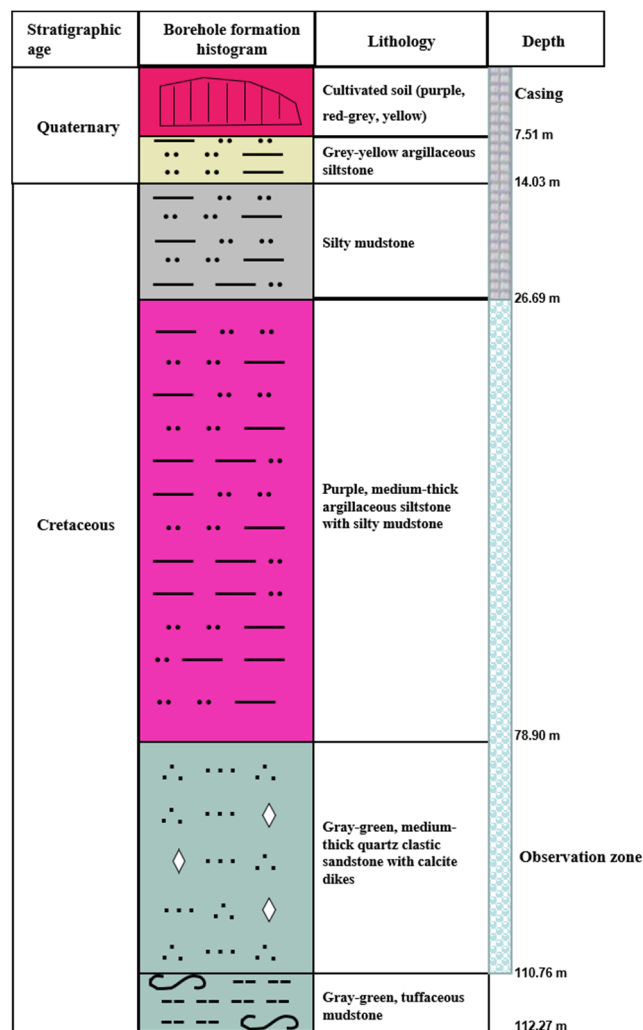


**Figure 2.** Schematic diagram of the Simao observation well borehole.

### 3. Methods

#### 3.1. Hydrochemical Observations

The Simao observation well hydrochemical data used in this study are daily data (measured at a fixed time of 8:00 (GMT +8)) from 1 January 2001 to 31 December 2018. The  $Mg^{2+}$  and  $Ca^{2+}$  concentrations were determined using the ethylene diamine tetraacetic acid (EDTA) volumetric method. The  $Ca^{2+}$  concentration was titrated with an EDTA standard solution at pH 12, while the combined  $Ca^{2+} + Mg^{2+}$  concentration was titrated with an EDTA standard solution at pH 10. The  $Mg^{2+}$  concentration was calculated using the subtraction method. The  $HCO_3^-$  concentration was determined by acid-base neutralization titration. Groundwater discharge was measured by the total amount method, in which water is collected in a measuring cup and the discharge is calculated based on volume and time.

#### 3.2. Hydrochemical Survey

In order to understand the anomaly mechanism of hydrochemical observations, or the relationship between ion changes of the observation well and the shallow water around it, additional water samples were collected from two shallow wells, a deep well, and two surface water sites (including a reservoir and a lake) near the Simao observation well. The neighboring deep well (from which a sample was collected in May 2018) is located 544 m from the Simao observation well; the source aquifer is at 117–197 m (i.e., deeper than that of the Simao observation well). The sample from the No. 1 shallow well was collected in May 2018; the well is 80 m from the Simao observation well. The sample from the No. 2 shallow well was collected in November 2016; the well is 500 m from the Simao observation well. Both of the shallow well aquifers are shallower than that of the Simao observation well. The lake and reservoir are 5 and 8 km from the observation well, respectively; samples were collected in November 2016. Water samples were filtered with 0.45- $\mu$ m filters and collected in two 100-mL polyethylene bottles. Ion concentrations were measured at the Institute of Earthquake Forecasting, China Earthquake Administration. Cation ( $K^+$ ,  $Na^+$ ,  $Mg^{2+}$ ,  $Ca^{2+}$ ). Anion ( $F^-$ ,  $Cl^-$ ,  $NO_3^-$ ,  $SO_4^{2-}$ ) concentrations were determined using a Dionex ICS-900 ion chromatographer (reproducibility within  $\pm 2\%$ );  $HCO_3^-$  concentrations were measured using standard titration procedures with a ZDJ-100 potentiometric titrator (reproducibility within  $\pm 2\%$ ).

#### 3.3. Seismic Activity

Studies have shown that hydrochemical anomalies can occur hundreds of kilometers from earthquake epicenters [46–49]. The Dobrovolsky et al. [50] formula is usually used to estimate the earthquake selection range of precursors and is expressed as:

$$R = 10^{0.43 M} \quad (1)$$

where  $R$  is the radius of the effective precursory manifestation area depending on the earthquake magnitude. We focused on the characteristics of geochemical anomalies before large earthquakes. According to the Dobrovolsky formula, the epicentral distance radius of  $M \geq 6$  earthquakes can reach 380 km. We expanded the scope of the study by including all  $M \geq 5$  earthquakes within a radius of 380 km around the Simao observation well. We identified 21 eligible earthquakes in the United States Geological Survey (USGS) database. However, we found that while all of the  $M \geq 5.6$  earthquakes caused sudden increases in groundwater discharge within 1 day, earthquakes of  $5.0 < M < 5.5$  were not associated with such changes. On this basis, we believe that variations in geochemical ion concentrations before  $M \geq 5.6$  earthquakes can effectively reflect tectonic genesis mechanisms. As a result, 10 earthquakes of  $M \geq 5.6$  with epicenters within 380 km of the Simao observation well were selected for inclusion in this study (Table 1).

**Table 1.** Earthquakes of  $M \geq 5.6$  within 380 km of the Simao observation well (2001–2018).

No.	Date	Location	Magnitude ( $M_W$ )	Longitude ( $^{\circ}$ E)	Latitude ( $^{\circ}$ N)	Epicentral Distance (km) <sup>a</sup>
1	21 July 2003	Dayao, China	6.0	101.290	25.975	362
2	16 May 2007	Laos	6.3	100.732	20.503	250
	2 June 2007	Ning'er, China	6.1	101.020	23.050	36
	23 June 2007	Myanmar	5.6	99.779	21.473	192
3	24 March 2011	Myanmar	5.7	99.770	20.650	267
	24 March 2011	Myanmar	6.9	99.822	20.687	261
4	7 October 2014	Jinggu, China	6.1	100.470	23.383	94
	5 December 2014	Jinggu, China	5.6	100.474	23.336	89
	6 December 2014	Jinggu, China	5.6	100.533	23.358	88
5	8 September 2018	Mojiang, China	5.7	101.578	23.332	86

<sup>a</sup> Distance from the Simao observation well.

According to their occurrence time, the earthquakes were divided into five groups. Groups 1 and 5 contain just one earthquake apiece (Figure 1 and Table 1). Groups 3 and 4 contain multiple earthquakes occurring in same area. In group 2, the three earthquakes occurred at similar times but in quite different locations (Figure 1 and Table 1). Groundwater discharge increased after both the Laos and Ning'er earthquakes of group 2; however, the change in discharge after the Ning'er earthquake was 3–4 times that of the Laos earthquake. This indicates that owing to its short (36 km) epicentral distance, the Ning'er earthquake had the greatest impact on the Simao observation well among the events in group 2. In group 3, the two earthquakes in 2011 were a foreshock ( $M$  5.7) and mainshock ( $M$  6.9). Group 4 contains a mainshock ( $M$  6.1) and two aftershocks. On this basis, the event times of the Dayao  $M$  6.0, Ning'er  $M$  6.1, Myanmar  $M$  6.9, Jinggu  $M$  6.1, and Mojing  $M$  5.7 earthquakes were used to mark the ends of the pre-seismic anomaly periods for each group.

## 4. Results

### 4.1. Hydrochemical Observations

Ion concentrations varied within relatively small ranges over the 18-year observation period (Figure 3);  $\text{Ca}^{2+}$  ranged from 35.1 to 41.2 mg/L,  $\text{Mg}^{2+}$  ranged from 6.0 to 8.3 mg/L, and  $\text{HCO}_3^-$  ranged from 201.6 to 313.5 mg/L. However, before the five groups of events,  $\text{Ca}^{2+}$ ,  $\text{Mg}^{2+}$ , and  $\text{HCO}_3^-$  exhibited obvious changes; the anomaly amplitudes had no significant relationship with seismic magnitude or epicentral distance. Furthermore, ion concentrations fell and then recovered or remained low until the earthquake occurred in each of the five groups. The start times and variations in amplitude of hydrochemical anomalies are listed in Table 2.

### 4.2. Atmospheric and Meteorological Conditions

Observations of atmospheric pressure and rainfall are available from 1 December 2003 (Figure 3). Atmospheric pressure shows a clear seasonal variation, but no relationship with ion concentrations (Figure 3). There is also no direct relationship between rainfall and ion concentrations; however, the rainy season may have some influence on the anomalies of different precursors, as discussed below.

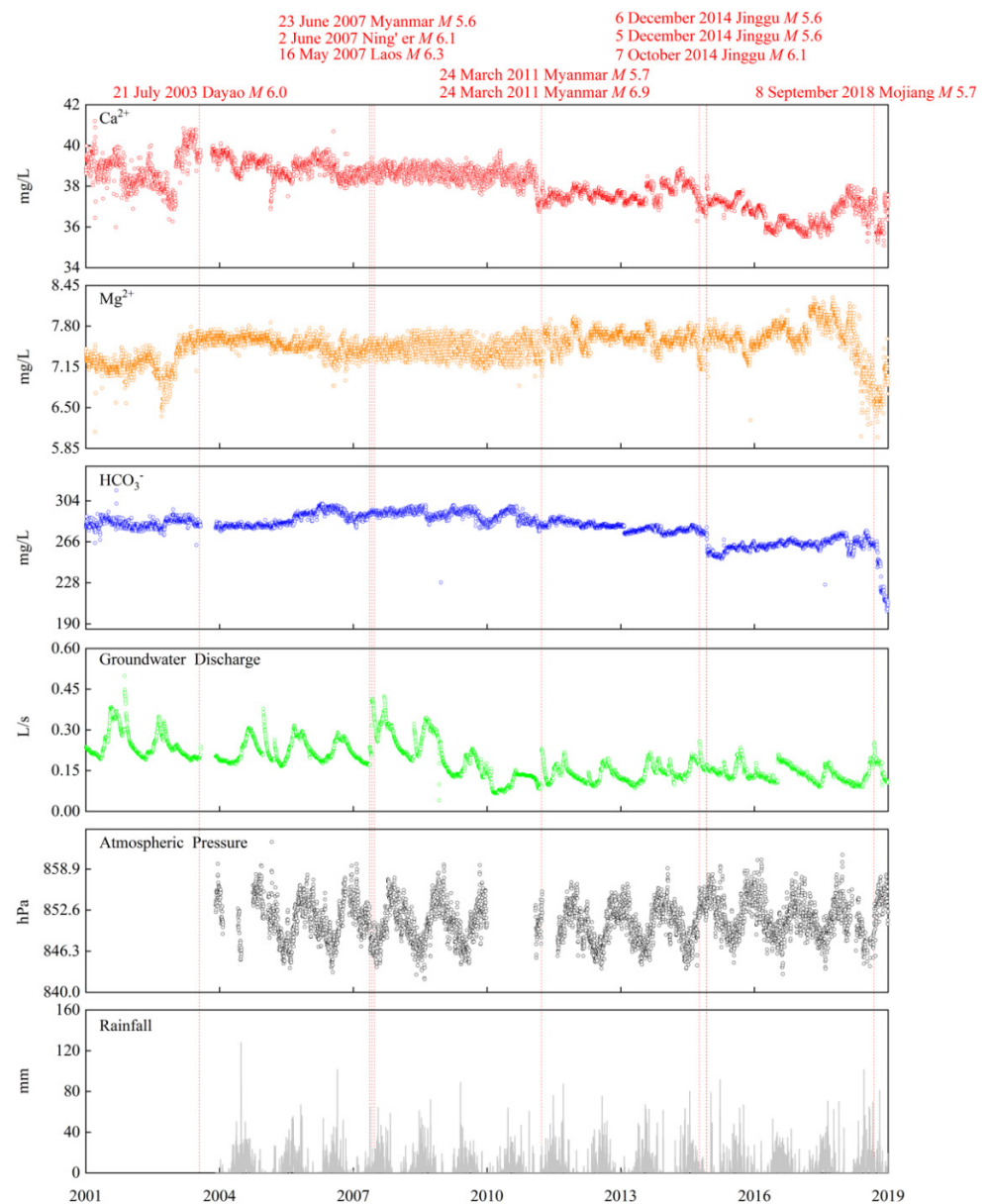


**Figure 3.** Time series of Ca<sup>2+</sup>, Mg<sup>2+</sup>, and HCO<sub>3</sub><sup>-</sup> concentrations (mg/L), along with groundwater discharge, atmospheric pressure, and rainfall at the Simao observation well from 2001 to 2008. The dates of  $M \geq 5.6$  earthquakes within a 380 km radius are marked by vertical red dashed lines.

#### 4.3. Hydrochemical Types

The hydrochemical type of the deep well sampled in 2018 is HCO<sub>3</sub>-Ca-Na. The hydrochemical types of all surface water sources are HCO<sub>3</sub>-Ca (including both shallow wells and the neighboring reservoir and lake). From the Schoeller diagram (Figure 4), the Simao observation well samples from 2016 and 2017 were consistent; there was a minor deviation in 2018, when the sample was collected in the period immediately before the Mojiang earthquake. Regardless, the data confirm that the Simao observation well aquifer and the deep well aquifer have the same material source; the lithologies of the two aquifers, and their water-rock reaction results are consistent. As such, ion concentrations in the deep well can be used as an endmember water source. This differs from the relationships between the ion concentrations of the Simao observation well aquifer and those of the other shallow water samples (Figure 4). The shallow aquifers and surface water are all able to enter the Simao observation well aquifer during tectonic movements, which could

be one of the main factors affecting the changing ion concentrations. A discussion of our results is based on the assumption that the deep and shallow aquifers represent the two endmembers of possible water sources.

**Table 2.** Pre-seismic hydrochemical variations in Simao observation well water <sup>a</sup>.

Earthquake	Dayao M 6.0		Laos M 6.3 Ning'er M 6.1 Myanmar M 5.6		Myanmar M 5.7 Myanmar M 6.9		Jinggu M 6.1 Jinggu M 5.6 Jinggu M 5.6		Mojiang M 5.7	
	Change	Time before event	Change	Time before event	Change	Time before event	Change	Time before event	Change	Time before event
Ca <sup>2+</sup>	↓ 7%	13 months	↓ 4.2%	12 months	↓ 5.9%	2 months	↓	2 months	↓ 7%	7 months
	↑ 9.2%	5 months	Low value maintained	10 months	Recovery	1 month	Recovery	1 month	Recovery	1 month
Precursory anomaly	↓	1 month			↓					
Mg <sup>2+</sup>	↓ 14%	12 months	↓ 10.8%	15 months	↓ 5.8%	2 months	↓ and recovery	15 days	↓	7 months
	↑ 21.9%	10 months	↑ 11.6%	9 months	Recovery	1 month				
HCO <sub>3</sub> <sup>-</sup>	↓	1 month			↓					
	↓ 4.5%	12 months	↓ 7.1%	12 months	↓ 6.4%	19 months	↓ 2.7%	21 months	↓ 7.6%	8 months
	↑ 8.4%	10 months	↑ 6.2%	6 months	Recovery	8 months	↓ 2.8%	11 months	Recovery	5 months
	↓	1 month			↓ 5.7%	6 months	↓	2 months		
					↓ 4.5%	1 month				

<sup>a</sup> Data for all earthquakes of M ≥ 5.6 within 380 km of the Simao observation well, Yunnan Province (2001–2018); ↓ without data denotes a change of less than 2%.

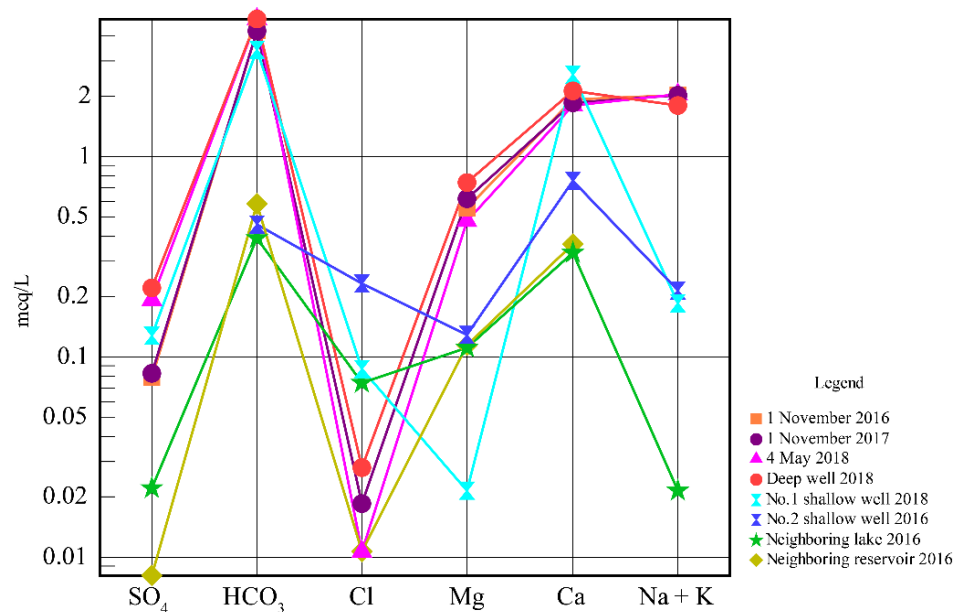


**Figure 4.** Schoeller diagram for samples from the Simao observation well, other nearby wells (one deep and two shallow), and local surface water. Data labelled using the day, month, and year of collection represent samples from the Simao observation well.

**5. Discussion**

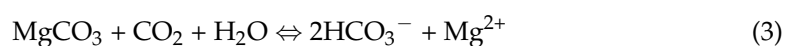
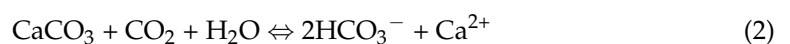
*5.1. Genetic Characteristics of Hydrochemical Precursors Due to CO<sub>2</sub> Injection*

Pre-seismic magmatic and tectonic activity is normally associated with the movement of deep crustal fluids [18,51–53]. Changes in hydrochemistry (i.e., ion concentrations) owing to gas release from deep fault zones or from intensified water-rock reactions before earthquakes have been observed [19,54,55]. Among these phenomena, CO<sub>2</sub> is the one of the

main gases released during seismic activity and is responsible for water-gas-rock interaction processes that can change the cation and anion concentrations of groundwater [4,56]. This CO<sub>2</sub> can be derived from three different sources: (1) mantle degassing and migration along faults; (2) degassing of carbonates in sedimentary rocks or water-rock interactions between brine and argillaceous rocks; and (3) biochemical CO<sub>2</sub> resulting from the decomposition of organic matter [57]. Owing to two small volcanic eruptions during the Quaternary [58], faults and CO<sub>2</sub>-rich fluid inclusions occur within the study area; the transport of CO<sub>2</sub> along strongly activated faults affects the chemical composition of groundwater. This response is much more significant than that caused by fluid migration.

Evidence from He-CO<sub>2</sub> systematics within hydrothermal gases reveals a mantle degassing extends to the localized magma degassing in the Simao blocks which is associated with Quaternary mantle-derived volcanism [41]. Mantle Helium proportion of the Simao samples reaches as high as 73% at hot springs which is less than 36 km from the observation well. Samples about 24 km far from the observation well show that  $\delta^{13}\text{C}_{\text{CO}_2}$  is  $-7.2\%$ , which is significant deep mantle source. The calculated carbon inventory from mantle is 62.8%, that from carbonate is 26.8%, and that from organic sediments is 10.4% [41]. Tectonic activities are one of the primary mechanisms for liberating deeply-sourced CO<sub>2</sub> from the Earth's interior to the surface [59]. CO<sub>2</sub> injection is thus the important process that can result in chemical changes during earthquake preparation in this observation well.

At the Simao observation well, the lithology of the main aquifer is a gray-green medium-thick quartz clastic sandstone with calcite dikes; the hydrochemical type of the water is HCO<sub>3</sub>-Ca·Na or HCO<sub>3</sub>-Na·Ca. Magnesium- and calcium-rich aquifers neutralize and trap injected CO<sub>2</sub> through the precipitation of calcite (CaCO<sub>3</sub>), dolomite (CaMg(CO<sub>3</sub>)<sub>2</sub>), and magnesite (MgCO<sub>3</sub>) [60]. Carbonate rocks interact with CO<sub>2</sub>, with the absorption of 1 mol of CO<sub>2</sub> producing 1 mol of Ca<sup>2+</sup> and Mg<sup>2+</sup>. Therefore, in an ideal state, the ratio of HCO<sub>3</sub><sup>-</sup> (mmol/L) to Ca<sup>2+</sup> + Mg<sup>2+</sup> (mmol/L) is always 2:1 based on carbonate weathering [61,62]. Assuming that observed pre-seismic changes in hydrochemistry result only from CO<sub>2</sub> injection, HCO<sub>3</sub><sup>-</sup> concentrations should be positively correlated with the Ca<sup>2+</sup> + Mg<sup>2+</sup> concentration (Equations (2) and (3)); however, owing to the relatively small amount of Mg<sup>2+</sup> in calcite [63], HCO<sub>3</sub><sup>-</sup> concentrations can also have a positive correlation with Ca<sup>2+</sup> only (Equation (2)).



As is shown in Table 1 and Figure 3, the earliest ions concentration variations before earthquakes are 21 months with HCO<sub>3</sub><sup>-</sup> concentrations. We compared the hydrochemistry of the observation well water from the 21 months decreasing until 2 months before the five groups of earthquakes in order to identify the correlation between HCO<sub>3</sub><sup>-</sup> and Ca<sup>2+</sup> + Mg<sup>2+</sup> concentrations, and that between HCO<sub>3</sub><sup>-</sup> and Ca<sup>2+</sup> concentrations as the result of CO<sub>2</sub> injection. We found correlations two months before some events (Figure 5). Three groups (groups 1, 3, and 4) had strong positive correlations, with changes in ion concentrations affected by CO<sub>2</sub> injection. Precursory anomalies caused by CO<sub>2</sub> injection occurred shortly before an earthquake series.

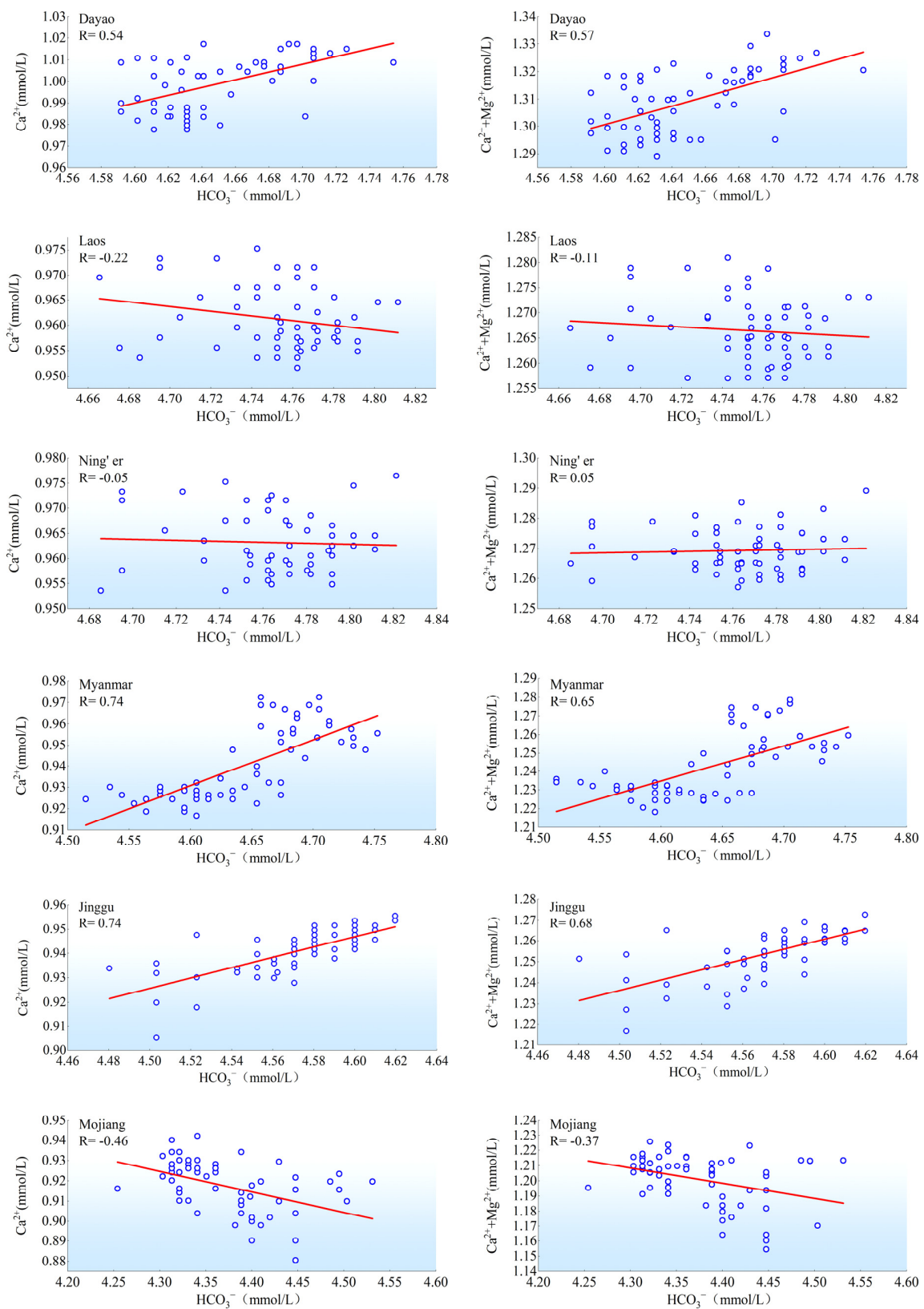


**Figure 5.** Relationships between  $\text{HCO}_3^-$  (mmol/L) and  $\text{Ca}^{2+}$  concentrations (mmol/L), and between  $\text{HCO}_3^-$  (mmol/L) and total  $\text{Ca}^{2+} + \text{Mg}^{2+}$  concentrations (mmol/L) in the 2-month period before five groups of earthquakes. Both the Laos and Ning'er earthquakes belong to group 2. The Laos earthquake was the earliest and largest event in group 2, while the Ning'er earthquake had the shortest epicentral distance. Blue circles denote pre-seismic data; red lines show the linear regressions through the data; 'R' is the correlation coefficient.

However, groups 2 and 5 did not show a correlation (Figure 5). Obviously, CO<sub>2</sub> injection is not the dominant reason causing the change of ion concentrations in these two groups before events. As we know, changes in ion concentrations can result from pre-seismic tectonic movement or from interference effects such as rainfall [4,32]. Comprehensive analysis of the magnitude, epicentral distance, number of earthquakes, and seasonal timings of the five groups with respect to precursory CO<sub>2</sub> injection shows that season has the most significant link in shorter epicentral distance. Groups 3 and 4 earthquakes occurred in the non-rainy season, and CO<sub>2</sub> injection was clearly the main factor in driving the precursory anomalies, regardless of epicentral distance, magnitude, or the number of earthquakes. Precursory anomalies controlled by CO<sub>2</sub> injection are characterized by significant decreases and recovery of Ca<sup>2+</sup>, Mg<sup>2+</sup>, and HCO<sub>3</sub><sup>-</sup> concentrations over a short period of time before the earthquakes (Figure 1 and Table 2). In contrast, the earthquakes in groups 1, 2, and 5 occurred during the rainy season, which anomaly mechanism was complex. Tectonic movement caused fault slip and pore fracture increased before events. Rainfall may accelerate its infiltration into the aquifers in the rainy season and cause the decreasing of ion concentrations, because the ion concentrations of rainwater are lower than those of the aquifers [37]. Furthermore, different aquifers could mix through tectonically created fissures formed within normally impermeable strata. Thus, the causes of precursory anomalies are more complex in the rainy season, which may be the result of the superposition of CO<sub>2</sub> injection, rainfall and mixing. For earthquakes that occurred during the rainy season and with epicentral distances within a radius of 250 km, CO<sub>2</sub> injection was not the main factor for precursory anomalies, regardless of the magnitude or number of earthquakes. However, before the Dayao earthquake, which had an epicentral distance of 362 km, CO<sub>2</sub> injection was the most significant cause of the precursory anomaly, although it was also affected by rainfall (Figure 5). Too far epicentral distance may weaken rainfall infiltration into the observation aquifers.

In summary, CO<sub>2</sub> injection could be the dominant fact to cause precursory anomalies of this observation well in 2 months before an earthquake series ( $M \geq 5.6$ ) in the non-rainy season, and the same with a far epicenter distance in rainy season. But, for a shorter epicenter distance, the combined effect of CO<sub>2</sub> injection, rainfall and mixing caused the decrease of Ca<sup>2+</sup>, Mg<sup>2+</sup> and HCO<sub>3</sub><sup>-</sup> concentrations due to tectonic movement in rainy season. However, the significant synchronous decrease of Ca<sup>2+</sup>, Mg<sup>2+</sup>, and HCO<sub>3</sub><sup>-</sup> concentrations in the observation well should be the signal for predicting  $M \geq 5.6$  earthquakes over a short time period in the study area.

### 5.2. Genetic Characteristics of Hydrochemistry Precursors Due to Mixing

Owing to southward clockwise rotation and extrusion of the Sichuan-Yunnan block, the Simao terrane has been compressed by the Sichuan-Yunnan block in a near NNE direction [64]. When the compressional load of a rock exceeds half of the compressive strength, the volume of the rock undergoes an inelastic increase (i.e., dilatancy) caused by micro-cracking. The dilatancy effect should be more pronounced around thrust faults [65]. Dilatancy may play an important role in triggering earthquakes [66], and earthquakes of this kind could show pre-seismic hydrochemical changes due to mixing between groundwater components [3,12,31,67]. For example, pre-seismic hydrogeochemical changes were recorded 1–10 weeks before the 2002  $M_w$  5.8 earthquake in Iceland [18]. In October 2012 and April 2013, pre-seismic hydrogeochemical changes were recorded 4–6 months before  $M_w$  5.5 and 5.6 events in Iceland [10].

Based on the research of permeability in the Simao observation well, there were significant permeability changes during the 2011  $M$  6.9 Myanmar earthquake and the 2014  $M$  6.1 Jinggu earthquake [45]. There was vertical flow exchange. The result of  $\delta D$  and  $\delta^{18}O$  from January to October in 2018 shows that the characteristics of mixing was significant during the September 2018  $M$  5.7 Mojiang earthquake [68]. For this study, cation concentration occurred the earliest anomalies in 15 months before earthquakes (Figure 3 and Table 2); as such, we took data from 450 days before each group to analyze the possible

mixing process. The hydrochemical types of the Simao observation well aquifer and the upper and lower aquifers represented by neighboring wells are dominated by  $\text{Ca}^{2+}$  and  $\text{HCO}_3^-$ . Based on the assumption that the main Simao aquifer is affected by inputs from both the upper and lower aquifers, we took data from the neighboring shallow wells and from the deep well to represent endmember mixing sources.  $\text{Ca}^{2+}$  and  $\text{HCO}_3^-$  were selected as coordinates, and data from 450 days before each of the five earthquakes were selected (Figure 6). The results confirm pre-seismic mixing before earthquakes, suggesting that the most likely mixing scenario is that of the aquifers feeding the deep well and the No. 2 shallow well; pre-seismic data for all five earthquakes are located near the tie-line between these two endmembers (Figure 6). The ratios of  $\text{Ca}^{2+}$  and  $\text{HCO}_3^-$  concentrations before the events in groups 1, 2, 3, and 5 fluctuate along the tie-line between the upper and lower aquifers, and likely reflect the mixing of the different aquifers (Figure 6). The precursory anomalies caused by mixing occurred very earlier before an earthquake series.

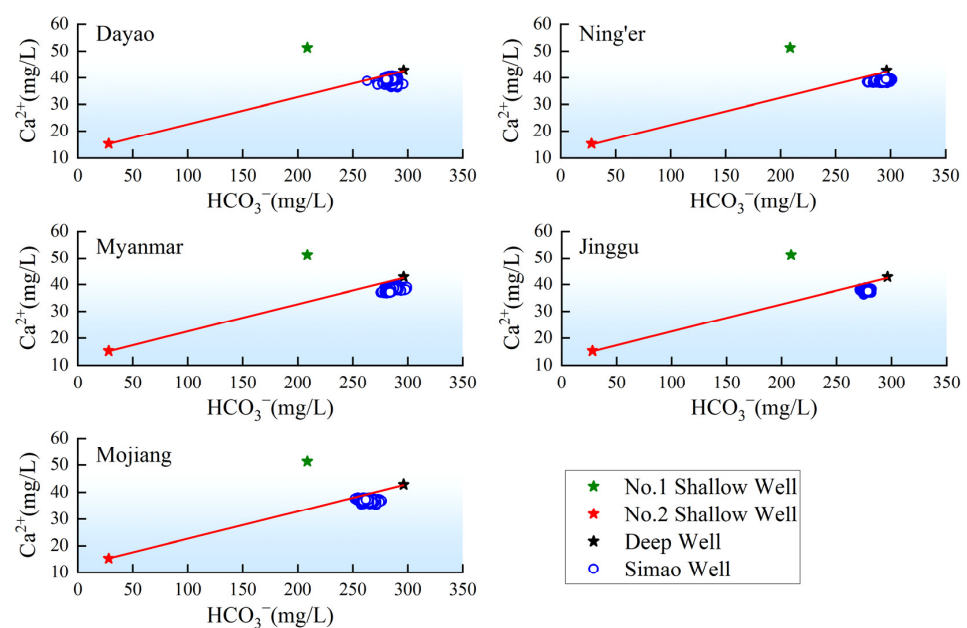


**Figure 6.** Relationships between  $\text{Ca}^{2+}$  and  $\text{HCO}_3^-$  concentrations among samples from a deep well, two shallow wells, and the Simao observation well. The Simao observation well data represent observations from 450 days before each of the five earthquake groups.

Moreover, the proportion of shallow water contributing to mixing is stable between 2003 and 2011. However, the  $\text{Ca}^{2+}$  and  $\text{HCO}_3^-$  concentrations deviated significantly from that of the deep well and approached to that of No.2 shallow well before Jinggu and Mojiang earthquakes (Figure 6). The proportion of shallow water contributing to mixing gradually increased significantly with the occurrence of 2014 Jinggu and 2018 Mojiang earthquakes. This should be the result of the regional strain field enhancement. The GPS velocity field during 2009–2013 and 2013–2017 were used to obtain the distributions of the main strain rate field and area strain rate field (Figure 7) using least-square collocation method in this region [69–71]. The results clearly show that the regional strain after 2013 was stronger than that before 2013. This also proved the result of hydrochemical mixing.

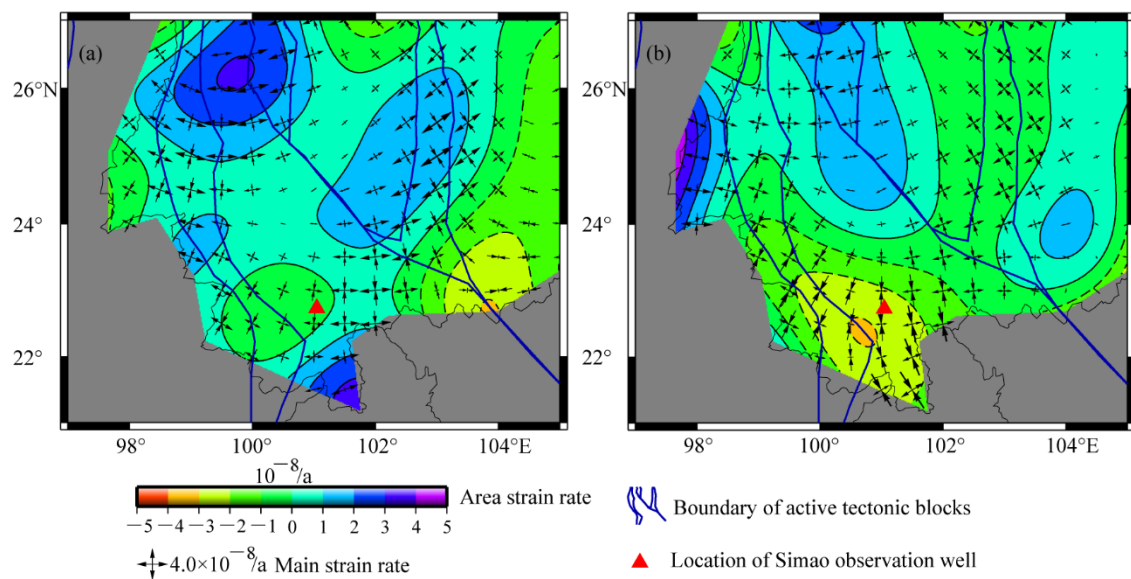


**Figure 7.** GPS main strain rate and area strain rate. (a) Results from 2009 to 2013; (b) Results from 2013 to 2017.

## 6. Conclusions

In this study, we analyzed an 18-year time series of hydrochemical data from the Simao observation well in the Lanping-Simao fault basin of southwest China. The results show that the CO<sub>2</sub> injection and groundwater mixing are both causes of regional  $M \geq 5.6$  earthquake precursors. CO<sub>2</sub> injection precursory anomaly caused a short-term hydrochemical variations before earthquakes due to its structure particularity in this well. The strong positive correlation ( $R > 0.5$ ) between Ca<sup>2+</sup> and HCO<sub>3</sub><sup>-</sup> concentrations could be catch the  $M \geq 5.6$  earthquake precursors in 2 months. The precursory anomalies caused by mixing occurred was a long-term hydrochemical variations with earliest to 15 months before an earthquake series. The proportion of shallow water contributing to mixing gradually increased significantly with the stronger regional strain after 2013. Overall, this study may provide a better understanding of two precursory mechanisms, CO<sub>2</sub> injection and groundwater mixing before  $M \geq 5.6$  earthquake in long-term observation well. This would be especially important for exploring possible hydrochemical precursory significant.

**Author Contributions:** Conceptualization, Z.Z. and H.F.; methodology, Z.Z.; software, J.Z. (Jun Zhong); validation, J.Z. (Jun Zhong), J.Z. (Jing Zhao), R.Y. and H.F.; formal analysis, J.Z. (Jing Zhao); investigation, L.T.; data curation, L.T.; writing—original draft preparation, Z.Z.; writing—review and editing, Z.Z.; visualization, J.Z. (Jun Zhong); funding acquisition, J.Z. (Jun Zhong), J.Z. (Jing Zhao) and Z.Z. All authors have read and agreed to the published version of the manuscript.

**Funding:** This research was funded by the National Key R&D Program of China [grant numbers 2018YFC1503606 and 2018YFE0109700], the National Natural Science Foundation of China [grant number 41503114], and the China Seismic Experimental Site [grant number 2019CSES0104].

**Data Availability Statement:** All data during the study are available from the corresponding author by request.

**Acknowledgments:** We thank Yuanze Duan for help during groundwater sampling. We thank the Assistant Editor Roy Li and two reviewers for constructive for comments and suggestions.

**Conflicts of Interest:** The authors declare that they have no conflict of interest.

## References

- Roeloffs, E. Hydrologic precursors to earthquakes: A review. *Pure Appl. Geophys.* **1988**, *126*, 177–209. [[CrossRef](#)]
- Skelton, A.; Liljedahl-Claesson, L.; Wästeby, N.; Andrén, M.; Stockmann, G.; Sturkell, E.; Mörth, C.M.; Stefansson, A.; Tollefsen, E.; Siegmund, H.; et al. Hydrochemical changes before and after earthquakes based on long-term measurements of multiple parameters at two sites in northern iceland—A review. *J. Geophys. Res. Solid Earth* **2019**, *124*, 2702–2720. [[CrossRef](#)]

3. Thomas, D. Geochemical precursors to seismic activity. *Pure Appl. Geophys.* **1988**, *126*, 241–266. [[CrossRef](#)]
4. Martinelli, G.; Dadomo, A. Factors constraining the geographic distribution of earthquake geochemical and fluid-related precursors. *Chem. Geol.* **2017**, *469*, 176–184. [[CrossRef](#)]
5. Tsunogai, U.; Wakita, H. Precursory chemical changes in ground water: Kobe earthquake, Japan. *Science* **1995**, *269*, 61–63. [[CrossRef](#)] [[PubMed](#)]
6. Claesson, L.; Skelton, A.; Graham, C.; Dietl, C.; Mörth, C.M.; Torssander, P.; Kockum, I. Hydrogeochemical changes before and after a major earthquake. *Geology* **2004**, *32*, 641–644. [[CrossRef](#)]
7. Song, S.; Ku, W.Y.; Chen, Y.; Liu, C.; Chen, H.F.; Chan, P.; Chen, Y.G.; Yang, T.; Chen, C.H.; Liu, T.; et al. Hydrogeochemical anomalies in the springs of the chiayi area in West-central Taiwan as possible precursors to earthquakes. *Pure Appl. Geophys.* **2006**, *163*, 675–691. [[CrossRef](#)]
8. Yuce, G.; Ugurluoglu, D.Y.; Adar, N.; Yalcin, T.; Yaltirak, C.; Streil, T.; Oeser, V. Monitoring of earthquake precursors by multi-parameter stations in Eskisehir region (Turkey). *Appl. Geochem.* **2010**, *25*, 572–579. [[CrossRef](#)]
9. Yaman, M.; Sasmaz, A.; Kaya, G.; Ince, M.; Karaaslan, N.M.; Özcan, C.; Akkus, S. Determination of elements in thermal springs for monitoring pre-earthquake activities by ICP-MS. *At. Spectrosc.* **2011**, *32*, 182–188. [[CrossRef](#)]
10. Skelton, A.; Andrés, M.; Kristmannsdóttir, H.; Stockmann, G.; Mörth, C.M.; Sveinbjörnsdóttir, Á.; Jónsson, S.; Sturkell, E.; Gudrunardóttir, H.; Hjartarson, H.; et al. Changes in groundwater chemistry before two consecutive earthquakes in Iceland. *Nat. Geosci.* **2014**, *7*, 752–756. [[CrossRef](#)]
11. Andrés, M.; Stockmann, G.; Skelton, A.; Sturkell, E.; Mörth, C.M.; Guðrúnardóttir, H.R.; Keller, N.S.; Odling, N.; Dahrén, B.; Broman, C.; et al. Coupling between mineral reactions, chemical changes in groundwater, and earthquakes in Iceland. *J. Geophys. Res. Solid Earth* **2016**, *121*, 2315–2337. [[CrossRef](#)]
12. Scholz, C.H.; Sykes, L.R.; Aggarwal, Y.P. Earthquake prediction: A physical basis. *Science* **1973**, *181*, 803–810. [[CrossRef](#)] [[PubMed](#)]
13. Nur, A. Matsushiro, Japan, earthquake swarm: Confirmation of the dilatancy-fluid diffusion model. *Geology* **1974**, *2*, 217–222. [[CrossRef](#)]
14. King, C.Y. Gas geochemistry applied to earthquake prediction: An overview. *J. Geophys. Res.* **1986**, *91*, 12269–12281. [[CrossRef](#)]
15. Muir, W.R.; King, G. Hydrologic signatures of earthquake strain. *J. Geophys. Res.* **1993**, *98*, 22035–22068. [[CrossRef](#)]
16. Rojstaczer, S.; Wolf, S.; Michel, R. Permeability enhancement in the shallow crust as a cause of earthquake-induced hydrological changes. *Nature* **1995**, *373*, 237–239. [[CrossRef](#)]
17. Du, J.G.; Amita, K.; Ohsawa, S.; Zhang, Y.L.; Kang, C.L.; Yanada, M. Experimental evidence on formation of imminent and short-term hydrochemical precursors for earthquakes. *Appl. Geochem.* **2010**, *25*, 586–592. [[CrossRef](#)]
18. Barberio, M.D.; Barbieri, M.; Billi, A.; Doglioni, C.; Petitta, M. Hydrogeochemical changes before and during the 2016 Amatrice–Norcia seismic sequence (central Italy). *Sci. Rep.* **2017**, *7*, 11735. [[CrossRef](#)]
19. Medici, G.; West, L.J.; Mountney, N.P. Characterization of a fluvial aquifer at a range of depths and scales: The Triassic St Bees Sandstone Formation, Cumbria, UK. *Hydrogeol. J.* **2017**, *26*, 565–591. [[CrossRef](#)]
20. Medici, G.; West, L.J.; Mountney, N.P.; Welch, M. Permeability of rock discontinuities and faults in the Triassic Sherwood Sandstone Group (UK): Insights for management of fluvio-aeolian aquifers worldwide. *Hydrogeol. J.* **2019**, *27*, 2835–2855. [[CrossRef](#)]
21. Silver, P.G.; Vallette-Silver, N.J. Detection of hydrothermal precursors to large northern California earthquakes. *Science* **1992**, *257*, 1363–1368. [[CrossRef](#)]
22. Zhang, W. *Research on Hydrogeochemical Precursors of Earthquakes*; Seismological Press 3: Beijing, China, 1994; pp. 170–182. (In Chinese with English abstract)
23. Roeloffs, E. Poroelastic techniques in the study of earthquake-related hydrologic phenomena. *Adv. Geophys.* **1996**, *37*, 135–195.
24. Wakita, H. Geochemical challenge to earthquake prediction. *Proc. Natl. Acad. Sci. USA* **1996**, *93*, 3781–3786. [[CrossRef](#)] [[PubMed](#)]
25. King, C.Y.; Azuma, S.; Igarashi, G.; Ohno, M.; Saito, H.; Wakita, H. Earthquake-related water-level changes at 16 closely clustered wells in Tono, central Japan. *J. Geophys. Res.* **1999**, *104*, 13073–13082. [[CrossRef](#)]
26. Toutain, J.P.; Baubron, J.C. Gas geochemistry and seismotectonics: A review. *Tectonophysics* **1999**, *304*, 1–27. [[CrossRef](#)]
27. Montgomery, D.; Manga, M. Streamflow and water well responses to earthquakes. *Science* **2003**, *300*, 2047–2049. [[CrossRef](#)]
28. Martinelli, G.; Ciolini, R.; Facca, G.; Fazio, F.; Gherardi, F.; Heinicke, J.; Pierotti, L. Tectonic-related geochemical and hydrological anomalies in Italy during the last fifty years. *Minerals* **2021**, *11*, 107. [[CrossRef](#)]
29. Binda, G.; Pozzi, A.; Michetti, A.M.; Noble, P.J.; Rosen, M.R. Towards the understanding of hydrogeochemical seismic responses in karst aquifers: A retrospective meta-analysis focused on the Apennines (Italy). *Minerals* **2020**, *10*, 1058. [[CrossRef](#)]
30. Wu, K.G. The Tectonic System and Genetic Mechanism Research of Simao Block in Yunnan Province. Ph.D. Thesis, China University of Geosciences, Beijing, China, 2006; pp. 1–56. (In Chinese with English abstract)
31. Reddy, D.V.; Kumar, D.; Rao, N.P. Long-term hydrochemical earthquake precursor studies at the Koyna-Warna reservoir site in Western India. *J. Geol. Soc. India.* **2017**, *90*, 720–727. [[CrossRef](#)]
32. Paudel, S.R.; Banjara, S.P.; Wagle, A.; Freund, F.T. Earthquake chemical precursors in groundwater: A review. *J. Seismol.* **2018**, *22*, 1293–1314. [[CrossRef](#)]
33. Wang, C.Y.; Manga, M. *Earthquakes and Water*; Springer: Berlin, Germany, 2010; p. 114.
34. Ingebritsen, S.; Manga, M. Earthquakes: Hydrogeochemical precursors. *Nat. Geosci.* **2014**, *7*, 697–698. [[CrossRef](#)]

35. Wang, Y.L.; Wang, L.C.; Wei, Y.S.; Shen, L.J.; Chen, K.; Yu, X.C.; Liu, C.L. Provenance and paleogeography of the Mesozoic strata in the Muang Xai Basin, northern Laos: Petrology, whole-rock geochemistry, and U–Pb geochronology constraints. *Int. J. Earth Sci.* **2017**, *106*, 1409–1427. [[CrossRef](#)]
36. Okamura, S.; Wu, G.Y.; Kagami, H.; Yoshida, T.; Kawano, Y. Geochemistry of Mesozoic intracontinental basalts from Yunnan, southern China: Implications for geochemical evolution of the subcontinental lithosphere. *Mineral. Petrol.* **1997**, *60*, 81–98. [[CrossRef](#)]
37. Zhang, Y.Q. Hydrogeochemical Characteristics and Genesis of the Springs in the Simao Basin of Yunnan. Doctor's Thesis, China University of Geosciences, Beijing, China, 2020. (In Chinese with English abstract).
38. Xue, C.J.; Chen, Y.C.; Wang, D.H.; Yang, J.M.; Yang, W.G. Geology and isotopic composition of helium, neon, xenon and metallogenic age of the Jinding and Baiyangping ore deposits, northwest Yunnan. *China Sci. China D* **2003**, *46*, 789–800. (In Chinese with English abstract) [[CrossRef](#)]
39. Dong, F.L.; Mo, X.X.; Hou, Z.Q.; Wang, Y.; Bi, X.M.; Zhou, S.  $^{40}\text{Ar}/^{39}\text{Ar}$  ages of Himalayan alkaline rocks in the Lanping basin, Yunnan and their geological significance. *Acta Petrol. Mineral.* **2005**, *24*, 103–109. (In Chinese with English abstract)
40. Chi, G.X.; Xue, C.J. Abundance of  $\text{CO}_2$ -rich fluid inclusions in a sedimentary basin-hosted Cu deposit at Jinman, Yunnan, China: Implications for mineralization environment and classification of the deposit. *Miner. Deposita.* **2011**, *46*, 365–380. [[CrossRef](#)]
41. Zhang, M.L.; Xu, S.; Zhou, X.C.; Caracausi, A.; Sano, Y.; Guo, Z.F.; Zheng, G.D.; Lang, Y.C.; Liu, C.Q. Deciphering a mantle degassing transect related with india-asia continental convergence from the perspective of volatile origin and outgassing. *Geochim. Cosmochim. Acta* **2021**, *310*, 61–78. [[CrossRef](#)]
42. Que, M.Y.; Chen, D.M.; Zhang, L.S.; Xia, W.J.; Zhu, C.Y. *Copper Deposits in the Lanping–Simao Basin*; Geological Publishing House: Beijing, China, 1998; p. 109. (In Chinese with English abstract).
43. Huang, J.G.; Ren, T.; Zou, H.J. Genesis of Xinzhai sandstone-type copper deposit in Northern Laos: Geological and geochemical evidences. *J. Sci.* **2019**, *30*, 95–108. [[CrossRef](#)]
44. Yang, Z.Z.; Deng, Z.H.; Zhao, Y.X.; Zhu, P.Y. Preliminary study on coseismic steps of water level in Dazhai well, Simao City, Yunnan Province. *Acta Seismol. Sin.* **2005**, *27*, 569–574. (In Chinese with English abstract) [[CrossRef](#)]
45. Hu, X.J.; Fu, H.; Li, T.; Li, Q. Study on co-seismic response and prediction significance of groundwater level in the Dazhai Well. *J. Seismol. Res.* **2020**, *43*, 341–347. (In Chinese with English abstract)
46. Hill, D.P.; Reasenber, P.A.; Michael, A.; Arabaz, W.J.; Beroza, G.; Brumbaugh, D.; Brune, J.N.; Castro, R.; Davis, S.; dePolo, D.; et al. Seismicity remotely triggered by the magnitude 7.3 landers, California, earthquake. *Science* **1993**, *260*, 1617–1623. [[CrossRef](#)]
47. King, C.Y.; Zhang, W.; Zhang, Z. Earthquake-induced groundwater and gas changes. *Pure Appl. Geophys.* **2006**, *163*, 633–645. [[CrossRef](#)]
48. Briestenský, M.; Thinová, L.; Praksová, R.; Stemberk, J.; Rowberry, M.D.; Knejřlová, Z. Radon, carbon dioxide and fault displacements in central Europe related to the Tōhoku earthquake. *Radiat. Rotect. Dosim.* **2014**, *160*, 68–82.
49. Jilani, Z.; Mehmood, T.; Alam, A.; Awais, M.; Iqbal, T. Monitoring and descriptive analysis of radon in relation to seismic activity of Northern Pakistan. *J. Environ. Radioact.* **2017**, *172*, 43–51. [[CrossRef](#)]
50. Dobrovolsky, I.P.; Zubkov, S.I.; Miachkin, V.I. Estimation of the size of earthquake preparation zones. *Pure Appl. Geophys.* **1979**, *117*, 1025–1044. [[CrossRef](#)]
51. Boschetti, T.; Barbieri, M.; Barberio, M.D.; Billi, A.; Franchini, S.; Petitta, M.  $\text{CO}_2$  inflow and elements desorption prior to a seismic sequence, Amatrice–Norcia 2016, Italy. *Geochem. Geophys. Geosyst.* **2019**, *20*, 2303–2317.
52. Barberio, M.D.; Gori, F.; Barbieri, M.; Billi, A.; Caracausi, A.; De Luca, G.; Franchini, S.; Petitta, M.; Doglioni, C. New observations in Central Italy of groundwater responses to the worldwide seismicity. *Sci. Rep.* **2020**, *10*, 1–10. [[CrossRef](#)]
53. Franchini, S.; Agostini, S.; Barberio, M.D.; Barbieri, M.; Billi, A.; Boschetti, T.; Pennisi, M.; Petitta, M. HydroQuakes, central Apennines, Italy: Towards a hydrogeochemical monitoring network for seismic precursors and the hydro-seismo-sensitivity of boron. *J. Hydrol.* **2021**, *598*, 125754. [[CrossRef](#)]
54. Bense, V.F.; Gleeson, T.; Loveless, S.E.; Bour, O.; Scibek, J. Fault zone hydrogeology. *Earth-Sci. Rev.* **2013**, *127*, 171–192. [[CrossRef](#)]
55. Caine, J.S.; Evans, J.P.; Forster, C.B. Fault zone architecture and permeability structure. *Geology* **1996**, *24*, 1025–1028. [[CrossRef](#)]
56. Ketzer, J.M.; Iglesias, R.; Einloft, S.; Dullius, J.; Ligabue, R.; Lima, V. Water-rock- $\text{CO}_2$  interactions in saline aquifers aimed for carbon dioxide storage: Experimental and numerical modeling studies of the Rio Bonito Formation (Permian), southern Brazil. *Appl. Geochem.* **2009**, *24*, 760–767. [[CrossRef](#)]
57. Ji, H.B.; Li, C.Y. Geochemistry of Jinman copper vein deposit, West Yunnan Province, China—II. Fluid inclusion and stable isotope geochemical characteristics. *Chin. J. Geochem.* **1998**, *17*, 81–90.
58. Zhao, C.P.; Wang, Y.; Ran, H.; Zhou, Z.; Chen, Y.L. Mantle-derived helium releasing in Southwestern Yunnan, China: Implications for M6 Cluster seismicity in Simao Puer seismic zone. *Recent Dev. World Seismol.* **2018**, *8*, 137–139. (In Chinese with English abstract)
59. Chiodini, G.; Cardellini, C.; Luccio, F.D.; Selva, J.; Ventura, G. Correlation between tectonic  $\text{CO}_2$  earth degassing and seismicity is revealed by a 10-year record in the apennines, Italy. *Sci. Adv.* **2020**, *6*, eabc2938. [[CrossRef](#)]
60. Gunter, W.D.; Perkins, E.H.; McCann, T.J. Aquifer disposal of  $\text{CO}_2$ -rich gases: Reaction design for added capacity. *Energy Convers. Manag.* **1993**, *34*, 941–948. [[CrossRef](#)]
61. Li, L.; Cao, J.H.; Huang, F.; Liang, Y.; Wang, P. Relation models of  $\text{Ca}^{2+}$ ,  $\text{Mg}^{2+}$  and  $\text{HCO}_3^-$  and analyses of carbon sinks influencing factors in the Chaotian river, Guilin. *Hydrogeol. Eng. Geol.* **2013**, *40*, 106–111. (In Chinese with English abstract) [[CrossRef](#)]

62. Zhong, J.; Li, S.L.; Liu, J.; Ding, H.; Sun, X.L.; Xu, S.; Wang, T.J.; Ellam, R.M.; Liu, C.Q. Climate variability controls on CO<sub>2</sub> consumption fluxes and carbon dynamics for monsoonal Rivers: Evidence from Xijiang River, Southwest China. *J. Geophys. Res. Biogeo.* **2018**, *123*, 2553–2567. [[CrossRef](#)]
63. Dong, A.G.; Zhu, X.K. Mg isotope geochemical cycle in supergene environment. *Adv. Earth Sci.* **2016**, *31*, 43–58. (In Chinese with English abstract)
64. Tong, Y.B.; Yang, Z.Y.; Wang, H.; Zhang, X.D.; An, C.Z.; Xu, Y.C.; Zhao, Y. The Cretaceous paleomagnetic results from the central part of the Simao Terrane in the southwest part of China and its tectonic implications. *Chin. J. Geophys. (Chin. Ed.)* **2014**, *57*, 179–198. (In Chinese with English abstract)
65. Sibson, R.H. Fluid flow accompanying faulting: Field evidence and models. *Earthq. Predict. Int. Rev.* **1981**, *4*, 593–603.
66. Sano, Y.; Takahata, N.; Kagoshima, T.; Shibata, T.; Onoue, T.; Zhao, D. Groundwater helium anomaly reflects strain change during the 2016 Kumamoto earthquake in Southwest Japan. *Sci. Rep.* **2016**, *6*, 1–7. [[CrossRef](#)] [[PubMed](#)]
67. Reddy, D.V.; Nagabhushanam, P. Chemical and isotopic seismic precursory signatures in deep groundwater: Cause and effect. *Appl. Geochem.* **2012**, *27*, 2348–2355. [[CrossRef](#)]
68. Li, Q.; Hu, X.J.; Fu, H.; Li, L.B.; Gao, W.F. Investigation and analysis on water quality anomalies of No. 17 well in Puer in Yunnan Province. *Plateau Earthq. Res.* **2019**, *31* (Suppl. 1), 64–71. (In Chinese with English abstract)
69. Wu, Y.Q.; Jiang, Z.S.; Yang, G.H.; Fang, Y.; Wang, W.X. The application and method of GPS strain calculation in whole mode using least square collocation in sphere surface. *Chin. J. Geophys.* **2009**, *52*, 1707–1714. (In Chinese with English abstract) [[CrossRef](#)]
70. Wu, Y.Q.; Jiang, Z.S.; Yang, G.H.; Wei, W.X.; Liu, X.X. Comparison of GPS strain rate computing methods and their reliability. *Geophys. J. Int.* **2011**, *185*, 703–717. [[CrossRef](#)]
71. Jiang, Z.S.; Liu, J.N. The method in establishing strain field and velocity field of crustal movement using least squares collocation. *Chin. J. Geophys.* **2010**, *53*, 1109–1117. (In Chinese with English abstract) [[CrossRef](#)]